Domain Formation in Phosphatidylcholine Bilayers Containing Transmembrane Peptides: Specific Effects of Flanking Residues †

ARTICLE *in* BIOCHEMISTRY · MARCH 2002

Impact Factor: 3.02 · DOI: 10.1021/bi011796x · Source: PubMed

9 AUTHORS, INCLUDING:

Hilde A. Rinia
Utrecht University
7 PUBLICATIONS **595** CITATIONS

SEE PROFILE

Josephine Antoinette Killian
Utrecht University
166 PUBLICATIONS **8,635** CITATIONS

SEE PROFILE

J.P.J.M. van der Eerden
Radboud University Nijmegen
120 PUBLICATIONS **2,721** CITATIONS

SEE PROFILE

Domain Formation in Phosphatidylcholine Bilayers Containing Transmembrane Peptides: Specific Effects of Flanking Residues†

Hilde A. Rinia,*,‡,§,|| Jan-Willem P. Boots,‡ Dirk T. S. Rijkers,⊥ Richard A. Kik,‡ Margot M. E. Snel,§ Rudy A. Demel,‡ J. Antoinette Killian,‡ Jan P. J. M. van der Eerden,§ and Ben de Kruijff‡

Institute of Biomembranes, CBLE, Department Biochemistry of Membranes, Utrecht University, Padualaan 8, 3584 CH, Utrecht, The Netherlands, Debye Institute, Department of Interfaces, Utrecht University, Padualaan 8, 3584 CH, Utrecht, The Netherlands, and Department of Medicinal Chemistry, Utrecht University, Sorbonnelaan 16, 3584 CA, Utrecht, The Netherlands

Received September 17, 2001; Revised Manuscript Received December 18, 2001

ABSTRACT: Lateral segregation in biological membranes leads to the formation of domains. We have studied the lateral segregation in gel-state model membranes consisting of supported dipalmitoylphosphatidylcholine (DPPC) bilayers with various model peptides, using atomic force microscopy (AFM). The model peptides are derivatives of the Ac-GWWL(AL)$_n$WWA-Etn peptides (the so-called WALP peptides) and have instead of tryptophans, other flanking residues. In a previous study, we found that WALP peptides induce the formation of extremely ordered, striated domains in supported DPPC bilayers. In this study, we show that WALP analogues with other uncharged residues (tyrosine, phenylalanine, or histidine at pH 9) can also induce the formation of striated domains, albeit in some cases with a slightly different pattern. The WALP analogues with positively charged residues (lysine or histidine at low pH) cannot induce striated domains and give rise to a completely different morphology: they induce irregularly shaped depressions in DPPC bilayers. The latter morphology is explained by the fact that the positively charged peptides repel each other and hence are not able to form striated domains in which they would have to be in close vicinity. They would reside in disordered, fluidlike lipid areas, appearing below the level of the ordered gel-state lipid domains, which would account for the irregularly shaped depressions.

Interactions between lipids and membrane proteins are generally known to have a major effect on the structure and function of biological membranes. An important aspect in the function and biogenesis of membrane proteins are the interactions between the amino acids flanking the hydrophobic transmembrane domain, and the hydrophobic−hydrophilic interfaces in the membrane.

It has been found that in integral membrane proteins with single- or multiple-spanning transmembrane helices, the interfacial region is enriched in aromatic residues (*1*−*3*). Especially tryptophans and tyrosines are abundant in the interface, and they are generally thought to have an anchoring (*4, 5*) and stabilizing (*6, 7*) function. Moreover, it has been suggested that aromatic residues are essential for the proper folding and assembly (*8*), and functioning of integral membrane proteins (*9, 10*). Tryptophan residues were found to be located at the hydrophobic side of the interfacial region, near the carbonyl/glycerol groups of the surrounding phospholipids (*5, 11*).

The positively charged residues lysine and arginine are enriched at the hydrophilic side of the interfacial region of transmembrane domains (*1, 7*) and in the segments flanking transmembrane α-helices (*2, 3*). Following the positive inside rule, they are preferentially located on the *cis*-side of membranes, (*12*), where they associate with anionic phospholipids (*13*), fulfilling a topology-determining role (*14*). When flanking a hydrophobic α-helix in transmembrane model peptides, lysines showed a distinct preference for the hydrophilic side of the interfacial region, close to the phosphate groups of the surrounding lipid bilayer (*5*).

To gain more insight in these interfacial interactions, model peptides have been used (*5, 15, 16*). An example of synthetic model peptides are the so-called WALP[1] peptides (*17*). These peptides consist of an alternating alanine-leucine stretch, forming a hydrophobic α-helix, which is flanked on both sides by two tryptophans.

Recently we have studied supported DPPC gel-state bilayers containing WALP peptides with atomic force microscopy [AFM (*18*)] (*19*). AFM offers the possibility to image supported bilayers under aqueous conditions with a high

† This work was supported by the Division of Chemical Sciences with financial aid from The Netherlands Organization for Scientific Research (N.W.O.).

* Correspondence should be addressed to this author.

‡ Institute of Biomembranes, Utrecht University.

§ Debye Institute, Utrecht University.

|| Current address: Lehrstuhl für Angewandte Physik, Ludwig-Maximilians-Universität München, Amalienstrasse 54, 80799, München, Germany. E-mail: hilde.rinia@physik.uni-muenchen.de.

⊥ Department of Medicinal Chemistry, Utrecht University.

[1] Abbreviations: DPPC, 1,2-dipalmitoyl-*sn*-glycero-3-phosphocholine; AFM, atomic force microscopy; WALP, Ac-GWWL(AL)$_n$WWA-Etn; GA, gramicidin A; CD, circular dichroism; DSC, differential scanning calorimetry; EM, electron microscopy; YALP, Ac-GYYL(AL)$_n$YYA-amide; FALP, Ac-GFFL(AL)$_n$FFA-amide; KALP, Ac-GKKL(AL)$_n$KKA-amide; HALP, Ac-GHHL(AL)$_n$HHA-amide; SP-C, surfactant protein C; TFE, trifluoroethanol; HAc, acetic acid; MLV, multilamellar vesicle; SUV, small unilamellar vesicle.

10.1021/bi011796x CCC: $22.00
Published on Web 01/30/2002

resolution (*20*−*22*). We found that the majority of the peptides segregated, together with some lipids, forming extremely ordered striated domains, in an otherwise predominantly flat bilayer. Overall, the length of the peptides and/or lipids did not influence this peculiar behavior. Previously, Mou and co-workers (*23*) found comparable results on gramicidin A (GA), which also clustered together with some lipids in ordered domains. Like WALP peptides, GA has tryptophan residues located at the hydrophobic−hydrophilic interface of the surrounding lipid bilayer.

To determine whether the formation of ordered striated domains is a general property of transmembrane peptides, or whether it is unique for peptides containing tryptophans as flanking residues, we have studied DPPC bilayers containing the WALP analogues YALP, FALP, KALP, and HALP. These peptides also consist of an alanine-leucine stretch, but are flanked by tyrosines, phenylalanines, lysines, or histidines, respectively, instead of tryptophans. Those amino acids are known to have different preferences for the hydrophobic−hydrophilic interface in membranes (*15*). Since these peptides share the same hydrophobic alanine-leucine segment, solely the effect of different flanking residues on the aggregation behavior of transmembrane peptides in DPPC bilayers could be determined. DPPC was chosen because DPPC bilayers have previously been extensively characterized by AFM and because it is a well-known, naturally occurring phospholipid, abundant in, for example, pulmonary lung surfactant.

We studied these systems with AFM and found that the peptides containing uncharged flanking residues were able to induce the formation of striated domains in supported DPPC bilayers, whereas the peptides containing positively charged residues induced homogeneously distributed, irregularly shaped depressions in the bilayer, and never striated domains. To explain this difference in morphology, circular dichroism (CD) and differential scanning calorimetry (DSC) measurements were done on several systems containing WALP analogues. To rule out that interactions between the bilayer and the substrate cause the observed morphology, freeze−fracture electron microscopy (EM) was performed on large multilamellar vesicles containing WALP or KALP. EM images of such vesicles showed bilayers with a morphology comparable to the supported bilayer systems.

MATERIALS AND METHODS

1,2-Dipalmitoyl-*sn*-glycero-3-phosphocholine (DPPC) was purchased from Avanti Polar Lipids (Alabaster, AL) and used without any further purification. WALP21, YALP21, and FALP21 consist of 21 amino acids in total. They contain a hydrophobic alanine-leucine stretch of 15 amino acids flanked on each side by 2 tryptophans, tyrosines, or phenylalanines, respectively. WALP23, KALP23, and HALP23 peptides consist of 23 amino acids, containing a hydrophobic alanine-leucine stretch of 17 amino acids flanked on each side by either tryptophans, lysines, or histidines. Table 1 shows the amino acid sequences of the different peptides we used. The N-terminus and C-terminus are blocked with an acetyl group and an ethanolamine or amide group, respectively. All peptides were synthesized essentially as described previously (*5*), and were >95% pure, as checked with HPLC. Porcine surfactant protein C (SP-C), consisting of 35 amino acids (sequence listed in Table 1), was isolated from lung lavage (*25*) and was a kind gift of Dr. E. J. A. Veldhuizen. 2,2,2-Trifluoroethanol (TFE) was from Sigma (St. Louis, MO). For all experiments, MilliQ water was used.

Table 1: Amino Acid Sequences of the Model Peptides and of Porcine SPC

peptide	amino acid sequence
WALP21	Ac-GWWL(AL)$_8$WWA-Etn
YALP21	Ac-GYYL(AL)$_7$YYA-amide
FALP21	Ac-GFFL(AL)$_7$FFA-amide
WALP23	Ac-GWWL(AL)$_8$WWA-Etn
KALP23	Ac-GKKL(AL)$_8$KKA-amide
HALP23	Ac-GHHL(AL)$_8$HHA-amide
porcine SPC[a]	*N*-L**R**IPCCPVDL**KR**LL(V)$_7$L(V)$_4$IVGALLMGL-*C*

[a] *N*-terminal cysteines are palmitoylated, postitively charged residues are denoted in boldface type, and the hydrophobic α-helical segment is underlined [from (*24*)].

Vesicle Preparation. The peptides were dissolved either in TFE or in a mixture of chloroform and methanol (3:1; v/v), both yielding similar results, and added to DPPC dissolved in a chloroform/methanol (3:1; v/v) mixture. The obtained peptide/lipid mixtures contained 1, 2, or 5 mol % peptide in lipid. These mixtures were dried in a rotary evaporator followed by overnight storage under high vacuum. To the dried mixed films was added 1.25 mL of 20 mM NaCl solution. In the case of the HALP23 peptides, a 10 mM Tris buffer with 20 mM NaCl, pH 9, or a 10 mM HAc buffer with 20 mM NaCl, pH 5, was used. For oriented CD measurements, pure MilliQ water was added. The hydrated film was shortly heated to 50 °C and vortexed, to promote vesicle formation. After 10 cycles of freeze−thawing (thawing at 50 °C), large multilamellar vesicles (MLVs) were obtained. Small unilamellar vesicles (SUVs) were made by sonicating a suspension of MLVs in a bath sonicator (Branson, Danburry, CT) at maximum power for at least 30 min, at 50 °C. Possible remaining large vesicles were spun down at 20800*g* for 1 h, at 4 °C. The supernatant containing SUVs was used for the preparation of supported bilayers.

Preparation of Supported Bilayers. The supported bilayers were prepared as described (*19*, *23*) using the vesicle fusion method. Briefly, 75 μL of SUV suspension with a lipid concentration of ±0.5 mM was applied onto freshly cleaved mica (o.d. 10 mm). The vesicles were allowed to adsorb to the mica for at least 10 h at 4 °C, as described (*23*). After rinsing (10 times with 75 μL of buffer), the sample was heated to 60 °C for 60 min, and afterward, the sample was left to cool to room temperature at ambient conditions and subsequently rinsed again. In this way bilayers were obtained, usually containing defects, piercing the bilayer, and with some unopened vesicles on top. Differences in lipid concentration in the SUV suspensions lead to different substrate coverages, which was optimized by prolonged or shortened adsorption times or additional heating and rinsing of the sample. This did not affect the observed morphology of the bilayers, but merely promoted the formation of large areas of bilayer without too many defects or unopened vesicles. The latter two yield features in the images, which disturb image processing with the AFM software. Supported bilayers of DPPC with 2 mol % of SPC incorporated were prepared following the above protocol; however, in this case, the SUV suspension had to be diluted 4 times before it was applied

to mica, to obtain a bilayer without too many unopened vesicles on top. All samples were scanned a few hours after preparation.

Atomic Force Microscopy. The sample was mounted on an E-scanner, which was calibrated on a standard grid, of a Nanoscope III (Digital Instruments, Santa Barbara, CA). A quartz flow cell was used without the O-ring. All samples were scanned with oxide-sharpened tips with a spring constant of 0.06 N/m, as estimated by the manufacturer (Digital Instruments, Santa Barbara, CA). Scans were recorded with a scan speed of 6 lines/s and at a minimal force where the image was stable and clear, which was usually smaller than 500 pN. All images shown are flattened raw data. All bilayers were imaged at room temperature.

Oriented Circular Dichroism. CD measurements on oriented lipid bilayers containing either WALP23 or KALP23 were performed following the procedure of de Jongh et al. (*26*). SUVs with a lipid concentration of ~5 mM with 2 mol % peptide in lipid, in MilliQ water, were prepared as described above. On a CD quartz cuvette, 60 μL of water was applied and subsequently heated to 60 °C. To the warm droplet was added 20−80 μL of vesicle suspension and kept at 60 °C under humid conditions for 20 min. Then the sample was left at 60 °C to dry, and after cooling, CD spectra were recorded on a Jasco J-600 spectropolarimeter with a scan speed of 20 nm/min, with 0.2 nm resolution, 1 nm bandwidth, and 1 s response time.

Differential Scanning Calorimetry. For DSC measurements, MLVs with a lipid concentration of 5.0 mM, prepared as described above, were used. The samples were degassed prior to use; 500 μL vesicles were injected in the sample cell of a MCS (Microcal Inc., Northampton, MA). Thermograms were recorded between 15 and 70 °C at a scan rate of 60 °C/h (upscan) and 45 °C/h (downscan).

Freeze−Fracture Electron Microscopy. Samples of MLVs with a lipid concentration of 10 mM with 2 mol % peptide in lipid were sandwiched between two hat-shaped copper holders and rapidly frozen in propane cooled in liquid nitrogen using a KF80 plunge freezing device (Reichert Jung, Vienna, Austria). After fracturing, platinum/carbon replicas were made in a BAF400 (Bal-tec, Baltzers, Liechtenstein). Replicas were observed with a CM10 Electron Microscope (Philips, Eindhoven, The Netherlands) operated at 80 kV.

RESULTS

Morphology of Supported Bilayers Containing Peptides. Images of pure DPPC bilayers as observed by AFM generally look smooth with defects piercing the bilayer (*19, 23, 27, 28*). Large defects can be used to measure the bilayer height, which is usually found to be 6 nm. This corresponds to the thickness of a gel-state DPPC bilayer with a thin layer of water, which is generally assumed to be present between the bilayer and the substrate (*21*). When examining these bilayers more closely, occasionally shallow cracks can be observed (*19*).

WALP peptides induce striated domains in supported DPPC bilayers (*19*), and this was found for peptides with a length of 19, 23, and 27 amino acids (WALP19, WALP23, and WALP27). An example of such a domain in a DPPC bilayer with 2 mol % WALP23 is given in Figure 1A, showing that the striated domains consist of ordered high (light) and low (dark) lines, with a repeat distance (i.e., the width of a low and a high line) of 7.5 ± 0.4 nm, which curve at angles of 120°.

Figure 1B depicts an image of a supported DPPC bilayer with 2 mol % WALP21 incorporated, also showing striated domains. The domains appear 2−3 Å above the level of the bilayer and consist of lines with a repeat distance of 7.6 ± 0.6 nm. In the gel-state bilayer outside the striated domains, line-type depressions can be seen, which were also observed for the WALPs with other lengths. They are thought to consist of disordered, fluidlike lipids and peptides being excluded from the solidified DPPC domains (*19*).

To determine whether these striated domains are only induced by peptides with a hydrophobic segment flanked by tryptophans, peptides containing other aromatic flanking residues were incorporated in DPPC bilayers and imaged by AFM. In YALP21, the flanking residues consist of tyrosines. In supported DPPC bilayers, containing 2 mol % YALP21, striated domains can be seen (Figure 1C). The lines in these domains have a repeat distance of 7.6 ± 0.4 nm; they are straight and seem to curve at defined angles (usually 120°).

Incorporation of FALP21, which has phenylalanines as flanking residues, also led to the formation of striated domains (Figure 1D), with a repeat distance of 8.2 ± 1.0 nm. The lines in these striated domains are curled and do not curve at defined angles.

Occasionally areas were observed appearing below the level of the bilayer. An example is given in Figure 1E, which shows a DPPC bilayer with 2 mol % YALP21. These lower areas sometimes appeared as flat roundish domains in the bilayer (Figure 1E), as thick lines, situated in the gel-state bilayer outside the striated domains (Figure 1E), and in the case of YALP21, also within the striated domains (not shown). Figure 1F shows the profile of this bilayer at the line drawn in Figure 1E. This height profile shows that these areas are approximately 2 nm below the surface of the bilayer. We assume that these lower areas consist of peptide and fluidized lipids, which would indeed appear about 2 nm below the level of a gel-state bilayer.

In conclusion, it can be said that apparently not only WALP peptides containing tryptophans as flanking residues, but also WALP analogues containing other aromatic residues have the ability to induce the formation of striated domains.

Another class of amino acids with the ability to anchor transmembrane segments are the positively charged lysines. KALP23 peptides consist of 23 amino acids in total, with the hydrophobic segment flanked by lysines. KALP23 has been shown to behave as if it has a hydrophobic length comparable to the shorter peptide WALP21, to the extent that they have the same mismatch-dependent destabilizing effect on the lamellar phase of liquid PCs (*5*). We found, however, that in DPPC bilayers, KALP23 peptides induce a completely different morphology than WALP peptides, and striated domains were never seen.

In DPPC bilayers with 2 mol % KALP23 incorporated, homogeneously distributed areas, appearing below the level of the bilayer, can be seen in the form of irregularly shaped small areas, meandering lines, and points. In Figure 2A, a 1 × 1 μm area of such a bilayer is depicted, and Figure 2E shows the height profile of the line drawn in the image of Figure 2A. The depth of the depressions depended on the

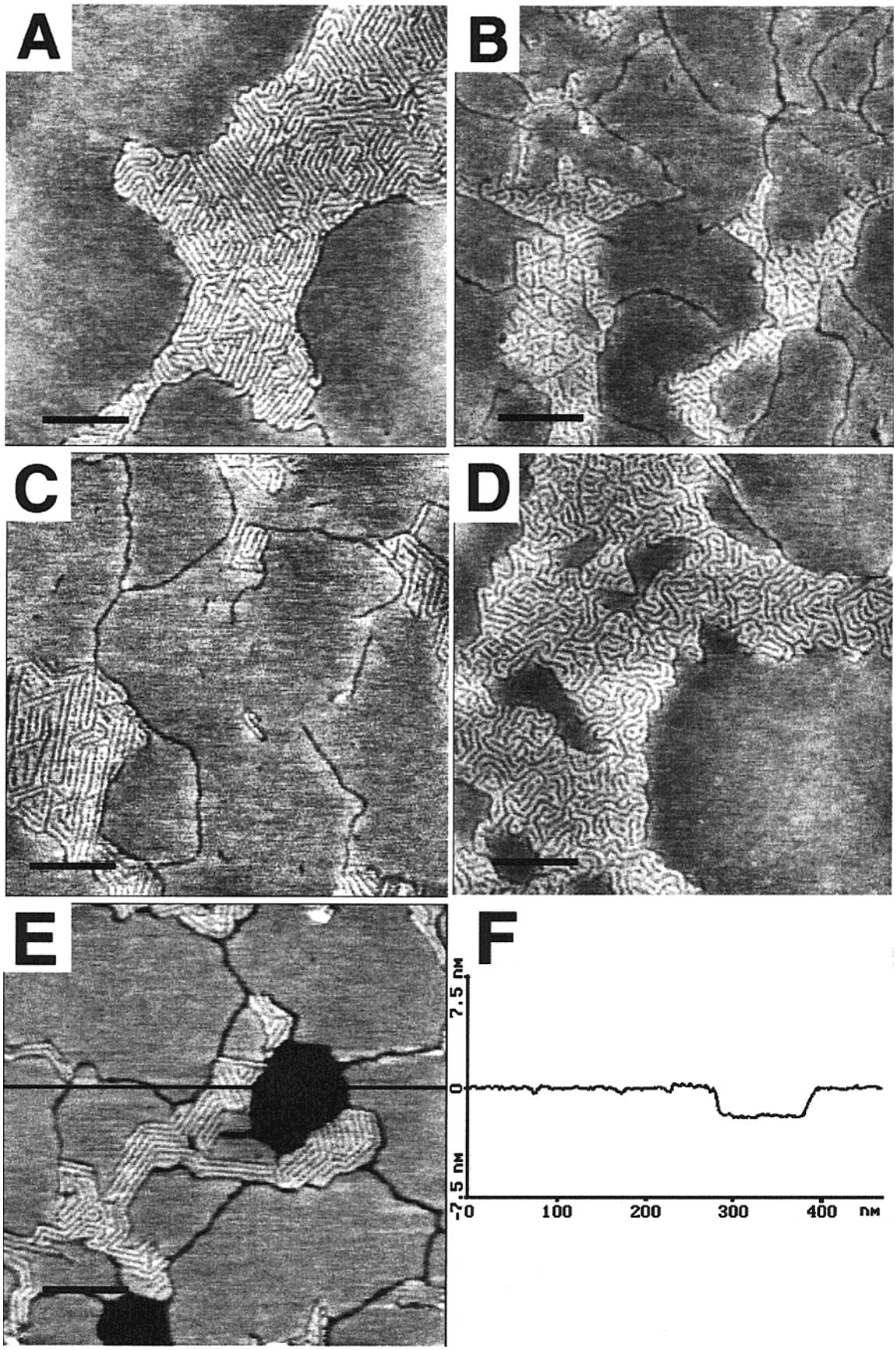

FIGURE 1: AFM images of striated domains induced in supported DPPC bilayers by uncharged model peptides. (A) DPPC with 2 mol % WALP23; (B) DPPC with 2 mol % WALP21; (C) DPPC with 2 mol % YALP21; (D) DPPC with 2 mol % FALP21; (E) occasionally lower areas were seen, as shown here for DPPC with 2 mol % YALP21; (F) cross section of the line drawn in (E). All bilayers are scanned in 20 mM NaCl. All scale bars are 100 nm.

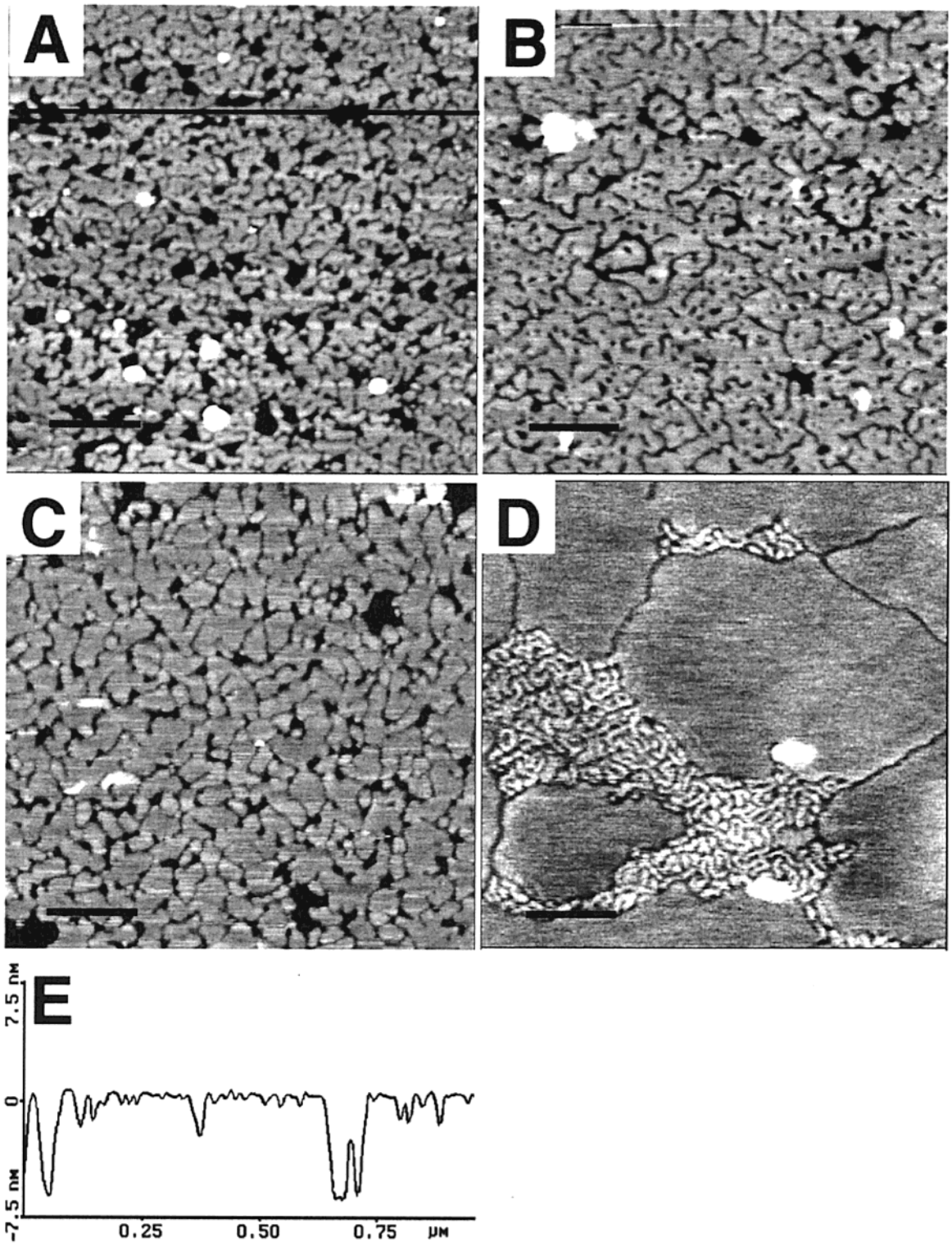

FIGURE 2: AFM images of supported DPPC bilayers with model peptides incorporated. (A) DPPC with 2 mol % KALP23, scanned in 20 mM NaCl, scale bar 200 nm; (B) DPPC with 1 mol % KALP23, scanned in 20 mM NaCl, scale bar 200 nm; (C) DPPC with 2 mol % HALP23, scanned in 10 mM HAc, 20 mM NaCl, pH 5, scale bar 200 nm; (D) DPPC with 2 mol % HALP23, scanned in 10 mM Tris, 20 mM NaCl, pH 9, scale bar 100 nm; (E) cross section of the line drawn in (A).

width of these depressions: the wider the holes, the deeper they were. The small holes and the point- and line-type depressions had a maximum depth of 1−2 nm. The largest holes had a depth of 6 nm, which indicates that at least in some cases the depressions pierce the bilayer.

When 1 mol % KALP23 was incorporated, again homogeneously distributed, irregular lower lines, small areas, and points were present, but the fraction of area appearing below the level of the bilayer was smaller (Figure 2B), compared to the bilayers with 2 mol % KALP23 (Figure 2A). In bilayers with 5 mol % KALP23, more irregular shaped lower areas were seen (data not shown) than in the bilayers with 2 mol % KALP23; thus, the fraction of lower area is dependent on the concentration of the peptide. Since the height

differences between the bilayer and the lower areas were small, it was not possible to quantify the amounts of lower area with the existing AFM software.

The morphology of bilayers containing peptides with lysines as flanking residues differs distinctly from the morphology of bilayers containing peptides with aromatic flanking residues (Figure 1). It could be that the observed difference is due to specific properties of lysines, or that positively charged residues in general induce the described morphology. To distinguish between these two possibilities, we studied HALP23. In HALP peptides, the flanking residues are histidines, which are protonated at low pH and deprotonated at high pH. These peptides offer the possibility to image bilayers with positively charged peptides (HALP at low pH) and bilayers with the same peptide, but uncharged (HALP at high pH).

In Figure 2C, a DPPC bilayer with 2 mol % HALP23 is shown, made and imaged at pH 5 (in HAc buffer). Under these circumstances, the HALP23 peptides are positively charged. Small irregular shaped areas and lines, and occasional points appeared below the level of the bilayer, yielding a morphology comparable to bilayers containing KALP23 peptides (Figure 2A).

Figure 2D depicts an image of a DPPC bilayer with 2 mol % HALP23, made and imaged at pH 9 (in Tris buffer). Uncharged HALP23 peptides give essentially the same results as the WALP23 peptides, in that line-type depressions are formed along with striated domains. The repeat distance of the lines in the striated domains is 8.5 ± 1.3 nm, which is comparable to the repeat distance of the lines in the domains induced by WALP23. However, as in the case of FALP21 (Figure 1D), the pattern formed by the lines in the striated domains induced by HALP23 is not as ordered as in the WALP23 domains (Figure 1A), and the lines seem more curled.

Bilayers containing WALP23 peptides, or KALP23 peptides made and scanned in the presence of the Tris buffer (pH 9) or HAc buffer (pH 5), always gave the same results compared to the ones obtained in the presence of 20 mM NaCl (Figures 1A and 2A). Thus, the observed difference in morphology of HALP23 containing bilayers at different pHs is not induced by the components of the buffers used.

In additional experiments, vesicles with 2 mol % HALP23 at pH 5 had been left to adsorb to mica, and subsequently the protocol was changed by rinsing the sample with Tris buffer (pH 9). After heating, rinsing, and scanning in Tris buffer, pH 9, striated domains were observed (data not shown). These domains were, however, smaller and more connected and homogeneously distributed than the ones observed in bilayers completely made and imaged at pH 9. When vesicles made and left to adsorb at pH 9 were subsequently treated with HAc buffer (pH 5), irregular cracks were observed in the bilayer surface, comparable to Figure 2C, occasionally together with large flat areas appearing 1−2 nm below the surface of the bilayer (data not shown). Apparently the formation of the striated domains could be manipulated by changing the pH, i.e., the charge of the HALP23 peptides, when the pH is changed before heating the adsorbed vesicles. When the pH was changed after the adsorbed vesicles had been heated, the bilayers became unstable, making it impossible to obtain clear and reproducible images.

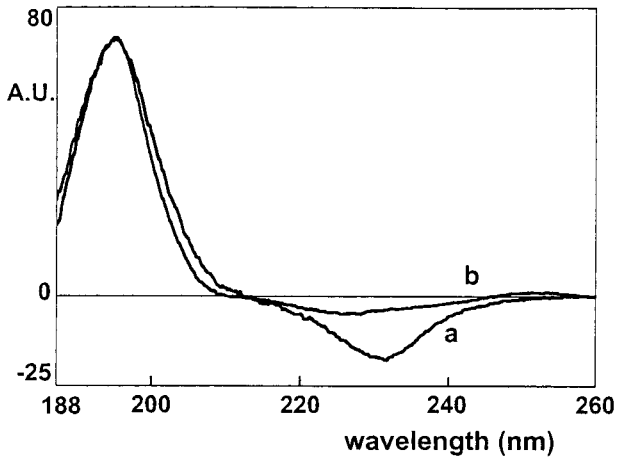

FIGURE 3: Circular dichroism spectra of 2 mol % WALP23 (a) and 2 mol % KALP23 (b) in oriented DPPC gel-state bilayers.

The morphology induced by KALP23 is not unique for lysine-flanked peptides, but is also induced by HALP23, when the histidine residues are positively charged. We also used AFM to study supported DPPC bilayers containing a naturally occurring, positively charged protein, pulmonary surfactant protein C (SP-C). This small hydrophobic, predominantly α-helical protein contains three positively charged residues (Table 1). Supported DPPC bilayers with 2 mol % SP-C incorporated also contained many irregularly shaped defects (data not shown), resembling the morphology of bilayers containing positively charged model peptides. Preliminary results on bilayers containing model peptides flanked by another positively charged residue, arginine, also gave comparable results (data not shown). Thus, we conclude that this morphology is typical for supported DPPC bilayers containing positively charged WALP analogues.

Since peptides with uncharged histidines as flanking residues can also induce the formation of striated domains, we propose that the induction of striated domain formation is typical for uncharged WALP analogues.

Orientation of Peptides in the Bilayer. WALP23 and KALP23 are known to adopt a transmembrane orientation in DMPC bilayers in the fluid phase (at 34 °C) (*5*); however, this is not necessarily the case in DPPC bilayers in the gel phase. To determine whether the observed difference in morphology induced by the uncharged and the charged peptides is due to a different orientation of the peptides in the bilayer (*29*), we performed CD measurements on oriented bilayers with WALP23 or KALP23 incorporated.

In Figure 3, CD spectra are shown of oriented lipid layers with a peptide concentration of 2 mol %. The spectra of both WALP23 (curve a) and KALP23 (curve b) show a maximum at 195 nm, while the crossover point is at 213 and 210 nm, respectively. This is characteristic for α-helices oriented parallel to the beam of incoming light and, in this case, perpendicular to the bilayer plane (*26*). In agreement with previous experiments with WALP23 and KALP23 incorporated in DMPC, the line-shape of the spectrum of WALP23 in oriented bilayers deviates somewhat from the spectrum of KALP23 in the 220−240 nm region, which is attributed to the tryptophan side-chain chromophores in WALP peptides (*5*).

According to our CD measurements, both WALP23 and KALP23 form an α-helix with a transmembrane orientation,

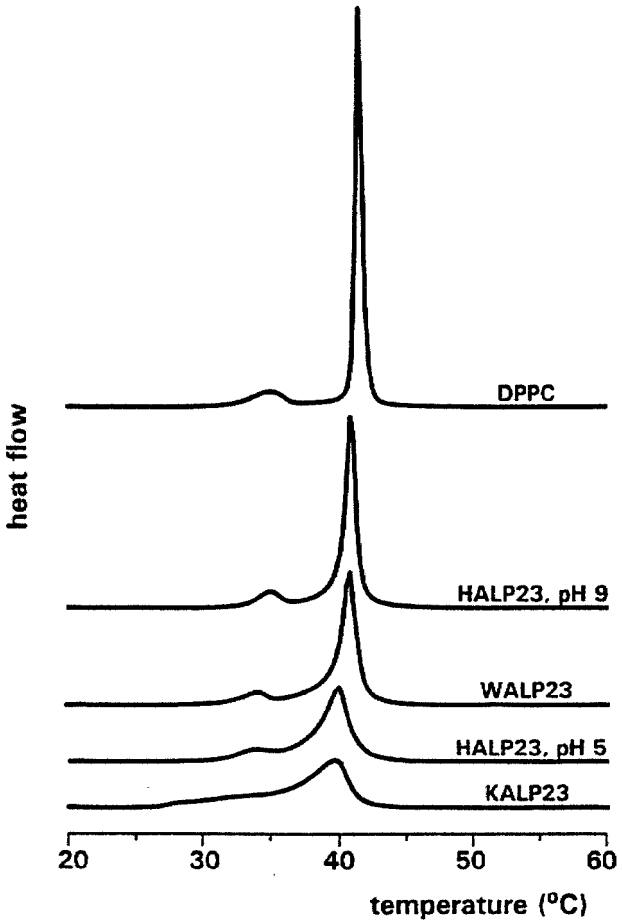

FIGURE 4: DSC heating curves of vesicles of (from top to bottom) pure DPPC in 20 mM NaCl; DPPC with 2 mol % HALP23 in 10 mM Tris, 20 mM NaCl, pH 9; DPPC with 2 mol % WALP23 in 20 mM NaCl; DPPC with 2 mol % HALP23 in 10 mM HAc, 20 mM NaCl, pH 5; and DPPC with 2 mol % KALP23 in 20 mM NaCl.

in planar DPPC gel-state bilayers. Thus, the observed difference in morphology between supported DPPC bilayers with uncharged and positively charged peptides is not due to a different orientation of the peptides in the bilayer.

Influence of Peptides on Lipid Thermotropic Phase Behavior. To understand how uncharged and charged peptides can induce such different morphology in DPPC bilayers, even though they both form a transmembrane α-helix, we aimed to obtain more insight in the peptide−lipid interactions of the different systems. Therefore, the effects of WALP23, KALP23, and HALP23 on the thermotropic phase behavior of DPPC were studied using differential scanning calorimetry (DSC) (*30*).

In Figure 4, the thermograms of DPPC vesicles containing 2 mol % WALP23, KALP23, or HALP23, at pH 9 and 5, are depicted, together with the thermogram of DPPC vesicles containing no peptide. The quantification of the thermodynamic parameters of these peptide/lipid and pure lipid systems is listed in Table 2.

The thermogram of pure DPPC shows a small, broad endothermic peak with a maximum at 35.1 °C, ascribed to the pre-transition, from the tilted solid to the ripple phase, and a large, narrow endothermic peak, with a maximum at 41.5 °C, ascribed to the main, ripple-to-fluid transition. This is characteristic for the phase behavior of DPPC (*31*).

Table 2: Thermodynamic Parameters of Pure DPPC and DPPC with 2 mol % Incorporated Model Peptides, As Measured with DSC

	no peptide	WALP23	HALP23, pH 9	KALP23	HALP23, pH 5
T_{tr} main (°C)	41.5	40.7	40.8	39.8	39.8
T_{tr} pre (°C)	35.1	33.9	34.7	−	33.8
$\Delta T_{1/2}$ main (°C)	0.6	1.7	0.8	4.0	2.5
enthalpy (%)	100	91	92	91	87

Thermograms of DPPC with uncharged peptides (WALP23 and HALP23 at pH 9) incorporated show a small downward shift of the main transition temperature, of less than 1 °C, and a small increase in width of the main endothermic peak ($\Delta T_{1/2}$). The relative enthalpy has decreased about 10%, compared to the pure lipids. These effects on the thermodynamic parameters are typical for the so-called type 3 proteins (*32*), indicating that the peptides mainly interact with the hydrophobic part of the lipid bilayer.

Thermograms of DPPC with positively charged peptides (KALP23 and HALP23 at pH 5) incorporated show a slightly larger downward shift of 1.7 °C and a significant increase in width of the main endothermic peak, compared to the uncharged peptides. The pre-transition peak of DPPC with HALP23 at pH 5 is also shifted to a lower temperature, while the pre-transition peak of DPPC with KALP23 incorporated has almost disappeared. As in the case of uncharged peptides, the relative enthalpy has decreased about 10%. This behavior is more like the behavior described for type 2 proteins (*32*), which indicates that the positively charged peptides also interact with the hydrophilic lipid headgroup region. The results we obtained on the positively charged peptides are comparable to the ones obtained by the group of McElhaney on similar peptides in saturated diacyl-PCs (*33*).

In conclusion, the DSC data show that both charged and uncharged peptides shift the phase transition temperatures of DPPC to lower values, which is indicative of a disordering effect of the peptides on the lipids. Furthermore, the DSC data indicate that the positively charged peptides disturb DPPC bilayers more than the uncharged peptides do.

Morphology of Vesicles Containing Peptides. The morphologies shown thus far have been observed in supported planar bilayers. To examine the possible influence of the solid support on the observed morphologies, we studied multilamellar vesicles containing 2 mol % WALP23 or KALP23. These vesicles were quenched from room temperature (below the main phase transition temperature), freeze-fractured, and imaged by electron microscopy (EM). Pure DPPC vesicles, as observed by freeze−fracture EM, showed smooth featureless planes (data not shown).

In the fracture plane of vesicles of DPPC with WALP23 incorporated, smooth featureless areas can be seen (denoted with a white arrow in Figure 5A), which are thought to be DPPC domains. Between these smooth areas, rough domains were observed. In some cases, in the structure of these domains, ordered lines were visible as shown in Figure 5A (denoted with a black arrow). The repeat distance of these lines was found to be 7.1 ± 0.8 nm, which is in excellent agreement with the repeat distance of the lines found in the striated domains in the supported bilayers. Hence, it can be said that the formation of ordered striated domains is a

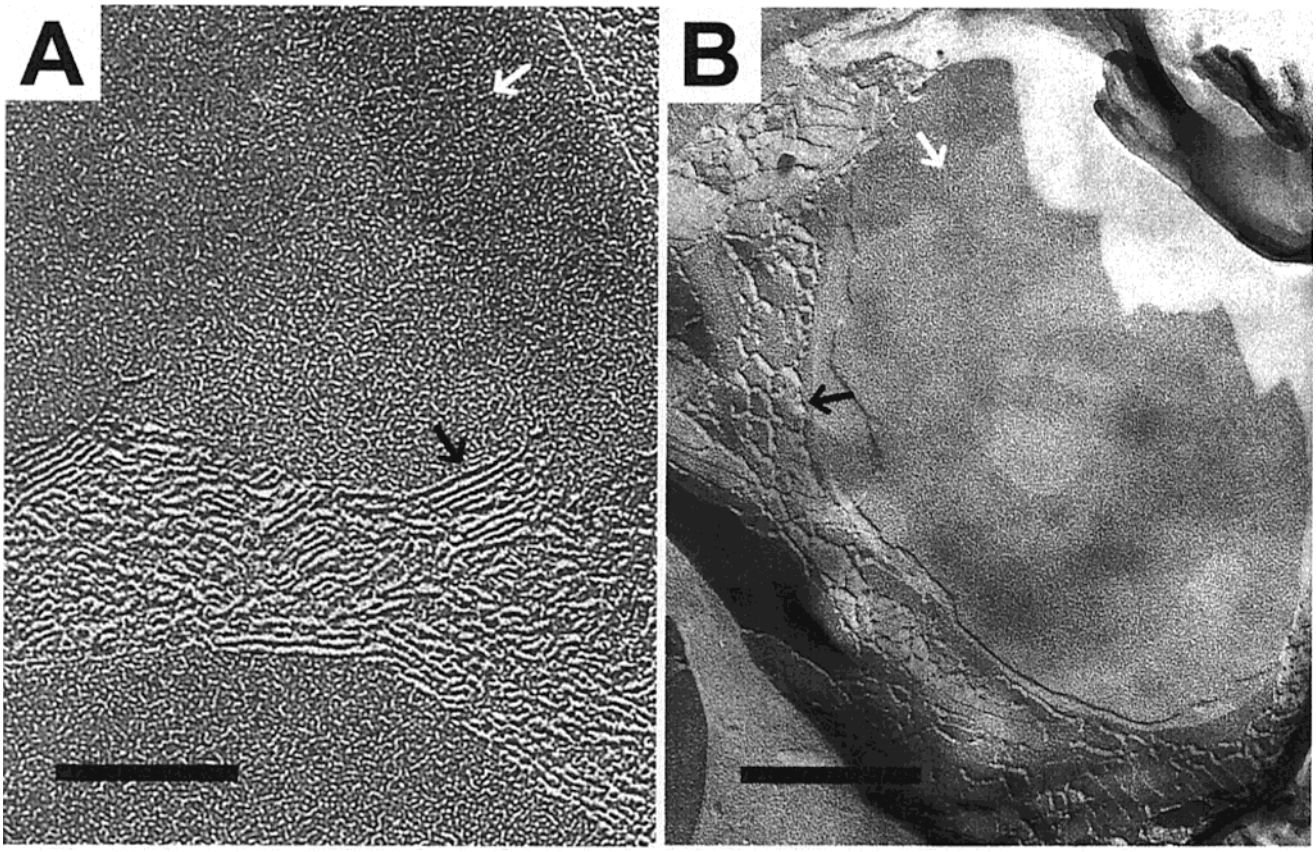

FIGURE 5: Electron microscopy images of freeze−fractured vesicles of (A) gel-state DPPC with 2 mol % WALP23, in 20 mM NaCl, scale bar 125 nm; and (B) gel-state DPPC with 2 mol % KALP23, in 20 mM NaCl, scale bar 250 nm.

characteristic feature of these peptide/lipid systems and is not induced by the substrate onto which the supported bilayers were deposited.

The fact that in the freeze−fractured vesicles the pattern of the domains seems not as ordered as in the supported samples, could be due to the ordering effect of mica, which has a hexagonal lattice, possibly directing the hexagonal order in the striated domains. However, if this were the case, all domains within one area should have their pattern lined up in the same direction, and this is not always the case. Furthermore, if mica could direct the order in the striated domains, also the domains in bilayers containing FALP21 and HALP23 (at high pH) should exhibit hexagonal order, which is, again, not the case. Instead, the amount of order in a striated domain seems to be dependent on the flanking residues and the length of the peptides.

Figure 5B depicts a fracture plane of a DPPC vesicle with 2 mol % KALP23 incorporated. In such vesicles, lines with a width of about 10 nm could be seen, with the same irregular pattern as observed for the supported bilayers containing 2 mol % KALP23 (Figure 2A), although the distance between the lines is larger. Furthermore, the lines are not homogeneously distributed through the bilayer, but clustered in large domains (denoted with a black arrow in Figure 5B). Outside these domains, smooth surfaces are visible (denoted with a white arrow in Figure 5B), presumably consisting of pure lipid domains. Domains as seen in the vesicles with WALP23 were never observed. Note that the scale bar in Figure 5A is 125 nm, and in Figure 5B, 250 nm.

DISCUSSION

We have imaged supported DPPC bilayers with incorporated model peptides containing various flanking residues. It was found that the uncharged peptides induce ordered, striated domains in which the peptides are thought to reside with some disordered lipids. The positively charged peptides induced irregularly shaped depressions. These morphologies were also seen with EM in unsupported systems. We will first discuss the morphology of bilayers containing uncharged model peptides, containing aromatic flanking residues, and then the morphology of bilayers containing positively charged flanking residues.

In a previous study, we showed that WALP peptides induce line-type depressions and striated domains in supported DPPC bilayers, and that the size and amount of the striated domains were dependent on the concentration of the peptide (*19*). In that study, we proposed a model of the molecular organization of both line-type depressions and the striated domains. Upon cooling the bilayer during the vesicle fusion protocol, from above to below the phase-transition temperature of DPPC, the lipids probably start to solidify at different "nucleation-sites" in the bilayer. This implies the formation of different lipid patches, and in one patch, the lipids could be tilted in a different direction than in another. In the boundaries between different lipid patches, the lipids are assumed to be in a disordered, fluidlike state. In pure DPPC bilayers, these boundaries are merely vaguely visible (*19*). In the presence of peptides, these peptides would be expelled from the rigidly packed, gel-state DPPC domains and end up in the boundaries between the patches, where

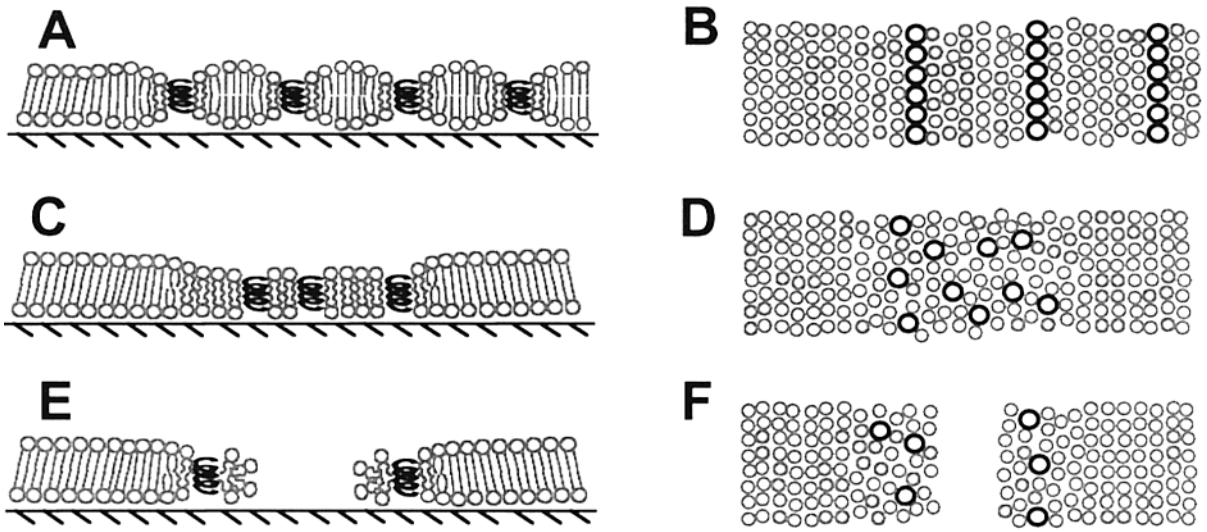

FIGURE 6: Proposed models for the molecular organization of bilayers with model peptides incorporated. The tilted packing of DPPC is disturbed by the presence of the peptides, depicted as black coiled springs. Uncharged peptides segregate, together with some lipids in striated domains in which peptide arrays flanked by fluidlike lipids appear as low lines, separated by less-tilted lipids, appearing as high lines in the AFM images. A cross section is depicted in (A), and (B) shows a top-view (lipids are depicted gray; peptides are depicted black). Charged peptides repel each other and thus cannot be forced in arrays. They either segregate with fluidlike lipids between the small gel-state patches (C, cross section; and D, top-view) or are accommodated in the disordered lipids, bordering holes that pierce the whole bilayer (E, cross section; and F, top-view).

the disordered, fluidlike lipids are present. In this case, the boundaries are clearly visible as line-type depressions. Excess peptide is thought to be accommodated in the striated domains, which increase in amount and size upon increasing peptide concentration (*19*). The striated domains would exist of arrays of peptide, flanked by disordered fluidlike lipids, forming the dark (low) lines in the striated domains in Figure 1A. These lines are thought to be separated by lipids, which are not as fluid as the lipids flanking the peptides, and hence may be solid enough to have straight acyl chains, but fluid enough to be less tilted than DPPC in the gel state. These lipids would appear above the level of the bilayer, which we assume is the explanation for the presence of the light (high) lines in the striated domains in Figure 1A. Figure 6A shows a cartoon of a cross section of this proposed model of the molecular organization in the striated domains (on the right) next to a gel-state lipid patch (left). Figure 6B depicts a top-view of this model. The results of the oriented CD measurements indicate that WALP23 peptides are indeed in a perpendicular orientation with respect to the plane of the membrane (Figure 3, line a). The finding with freeze−fracture EM, that in unsupported DPPC systems containing WALP23, also striated domains are present (Figure 5A), with a repeat distance of 7.1 ± 0.8 nm, shows that the striated domains are not induced by the support onto which the bilayers are deposited. This also is in agreement with the proposed model.

The proposed model involves the preference of the peptides to be surrounded by lipid, while the lipids, due to their tight packing in the gel phase, prefer to stay together. The resulting compromise is the formation of lines, clustered together in striated domains. The mechanism underlying this model implies that the formation of the striated domains is nonspecific for the peptide. This is supported by the finding of Mou et al. (*23*) that gramicidin A (GA) also induces the formation of ordered domains. However, since both GA and WALP peptides contain tryptophans as flanking residues, the possibility exists that line formation is induced by stacking interactions between tryptophans of neighboring peptides. However, peptides with other uncharged flanking residues [tyrosine, phenylalanine, and histidine (at high pH), Figures 1C and 1D, and 2D] also induce the formation of striated domains, indicating that no such stacking interactions are involved, and illustrating the nonspecificity of the underlying mechanism. We propose that the molecular organization of both line-type depressions and the striated domains, present in bilayers containing YALP21, FALP21, and HALP23 (high pH), as depicted in Figures 1C and 1D, and 2D, is the same as in bilayers containing WALP peptides (see also Figure 6A).

The pattern of the striated domains induced by WALP21, WALP23, and YALP21 resembles the ripple phase in that it consists of ripples, and exhibits 3-fold symmetry. However, since the repeat distance remains constant upon changing the length of the peptides or lipids, it was concluded previously (*19*) that the striated domains do not correspond to the ripple phase, or any other modulated phase (*34*). Moreover, on some samples a second bilayer on top of the first bilayer was observed, exhibiting a ripple-phase structure, with different repeat distances and morphology compared to the striated domains (Rinia et al., unpublished observations). Second bilayers have been found more often to show ripple-phase structures (*23, 35*).

The pattern varies for peptides with different flanking residues. WALP21, WALP23, and YALP21 form domains with straight lines, curving at defined angles (Figure 1A−C). The flanking residues of these peptides, i.e., tryptophan and tyrosine, are known to preferentially locate at a specific position in the membrane interface (*36*), and have a "strong" anchoring potency (*37*). Striated domains containing FALP21 and HALP23 (at high pH) consist of curled lines, curving at less defined angles (Figures 1D and 2D). The flanking residues of these peptides, e.g., phenylalanine and histidine, were found to anchor less strongly compared to tryptophan

and tyrosine (*37*). Although the exact mechanism is not understood, we suggest that there is a correlation between the anchoring function of the flanking residues of the peptides and the order in the pattern of the striated domains induced by these peptides. The effect of the geometry of the involved molecules and the difference in tilt between the peptides and the lipids on the formation of striated phases will be investigated soon by using Monte Carlo computer simulations (*38*).

Supported DPPC bilayers with KALP23 or HALP23 (at low pH) give rise to a completely different morphology compared to bilayers with uncharged peptides. Striated domains were never seen. Since both KALP23 and HALP23 (at low pH) are positively charged, and since HALP23 at high pH, when it is uncharged, did induce the formation of striated domains, we propose that the different morphology, as seen for KALP23 and HALP23 at low pH, is due to the positive charges of the flanking residues. These charges would cause the peptides to repel each other, and therefore the peptides cannot form striated domains in which they would have to be in close vicinity.

DPPC bilayers containing 2 mol % KALP23 show pointlike and irregularly shaped line-type depressions along with irregularly shaped lower areas, all homogeneously distributed over the bilayer (Figure 2A). In bilayers with 1 mol % KALP23 (Figure 2B) and 5 mol % KALP23 (data not shown), also pointlike and line-type depressions and lower areas can be seen, but less and more, respectively, compared to bilayers with 2 mol % KALP23. Apparently the depressions are dependent on the concentration of the peptide. According to the CD measurements, the peptides are present in a perpendicular orientation with respect to the plane of the bilayer (Figure 3, line b). Since both KALP23 and HALP23 (3.6 nm) are shorter than the thickness of a DPPC gel-state bilayer [4.7 nm (*39*)], logically they would appear below the level of the bilayer. From this, we deduce that KALP23 and HALP23 are located in or at the edges of the depressions.

We could not determine the depth of the points, lines, and lower areas unambiguously, since the depth seemed to vary with the width of the depressions, most probably because the tip is not sharp enough to completely reach "the bottom" of narrow holes. This means that all the depressions could be as deep as the whole bilayer, as seen for the large depressions (Figure 2E). On the other hand, it could also be that the depths of the pointlike and line-type depressions are indeed merely 1−2 nm deep.

In the case that the pointlike and irregular line-type depressions are about 1−2 nm deep, then these lines most probably consist of disordered fluidlike lipids, in which the peptides are dissolved. The positively charged peptides are separated by the fluidlike lipids. This organization is depicted as a cross-section in Figure 6C, and as a top-view in Figure 6D.

In the case that all the lower areas pierce the entire bilayer, the charged peptides would be situated in the edges of the bilayer, bordering the aqueous phase in the hole through the bilayer. These edges are assumed to consist of lipids oriented such that the hydrophilic headgroups shield the hydrophobic acyl chains from the aqueous phase, as depicted in Figure 6E (*27, 28*). To make this curve, the lipids cannot be in the tightly packed gel state, but have to be disordered. It should be the most favorable for the peptides to reside in these disordered sites (Figure 6E). A top-view of this organization is depicted in Figure 6F.

In both cases, the bilayer is fragmented in small domains of gel-state lipids. This would decrease the cooperativity of a phase transition of such a bilayer, and this is reflected in the large $\Delta T_{1/2}$ of the phase transition of DPPC vesicles containing positively charged peptides.

Freeze−fracture EM of vesicles containing 2 mol % KALP23 revealed meandering lines and occasionally points in the bilayer. If these lines and points correspond to the line-type and pointlike depressions as seen in the AFM images, it is most likely that in these lines and points peptides are/were residing. This suggests that the molecular organization of the pointlike and line-type depressions in bilayers containing positively charged peptides is most likely as depicted in Figure 6B.

Although the EM images of DPPC vesicles with WALP23 incorporated closely resemble the AFM images of the same systems on mica, the EM results on DPPC vesicles containing KALP23 differ from the AFM images of supported DPPC bilayers with KALP23. In the vesicles containing KALP23 (Figure 5B), the lines are present in domains outside smooth areas of, most likely, pure lipid, whereas in the supported systems, the irregular line-type depressions are homogeneously distributed over the bilayer (Figure 2A). We suspect that the negative charges of the substrate cause this distribution of the positively charged peptides. However, since shielding of the charges, by preparing and scanning supported bilayers with incorporated KALP23 in the presence of 10 mM Mg^{2+}, also yielded bilayer homogeneously distributed depressions (data not shown), the exact cause of this observed difference remains unclear.

In conclusion, the results of this study show unexpected abilities of transmembrane model peptides. In DPPC bilayers, they organize in domains with characteristic morphologies. The remarkably different effects of positively charged versus uncharged aromatic residues demonstrate the specific ways those residues determine the interactions of transmembrane peptides with lipids.

ACKNOWLEDGMENT

We thank G. J. K. van den Berg for skillful technical assistance, Drs. R. E. Koeppe II and D. V. Greathouse for providing us with WALP21 and WALP23, and Dr. E. J. A. Veldhuizen for providing us with SP-C.

REFERENCES

1. Landolt-Marticorena, C., Williams, K. A., Deber, C. M., and Reithmeier, R. A. F. (1993) *J. Mol. Biol. 229*, 602−608.
2. Reithmeier, R. A. F. (1995) *Curr. Opin. Struct. Biol. 5*, 491−500.
3. von Heijne, G. (1994) *Annu. Rev. Biophys. Biomol. Struct. 23*, 167−192.
4. Braun, P., and von Heijne, G. (1999) *Biochemistry 38*, 9778−9782.
5. de Planque, M. R. R., Kruijtzer, J. A. W., Liskamp, R. M. J., Marsh, D., Greathouse, D. V., Koeppe, R. E., II, de Kruijff, B., and Killian, J. A. (1999) *J. Biol. Chem. 274*, 20839−20846.
6. Woolf, T. B. (1997) *Biophys. J. 73*, 2376−2392.
7. Ridder, A. N. J. A., Morein, S., Stam, J. G., Kuhn, A., de Kruijff, B., and Killian, J. A. (2000) *Biochemistry 39*, 6521−6528.

8. Schiffer, M., Chang, C.-H., and Stevens, F. J. (1992) *Protein Eng. 5*, 213−214.
9. Becker, M. D., Greathouse, D. V., Koeppe, R. E., II, and Andersen, O. S. (1991) *Biochemistry 30*, 8830−8839.
10. Hu, W., and Cross, T. A. (1995) *Biochemistry 34*, 14147−14155.
11. Yau, W.-M., Wimley, W. C., Gawrisch, K., and White, S. H. (1998) *Biochemistry 37*, 14713−14718.
12. von Heijne, G. (1986) *EMBO J. 5*, 3021−3027.
13. van Klompenburg, W., Nilsson, I., von Heijne, G., and de Kruijff, B. (1997) *EMBO J. 16*, 4261−4266.
14. von Heijne, G. (1989) *Nature 341*, 456−458.
15. Wimley, W. C., and White, S. H. (1996) *Nat. Struct. Biol. 3*, 842−848.
16. Mall, S., Broadbridge, R., Sharma, R. P., Lee, A. G., and East, J. M. (2000) *Biochemistry 39*, 2071−2078.
17. Killian, J. A., Salemink, I., de Planque, M. R. R., Lindblom, G., Koeppe, R. E., II, and Greathouse, D. V. (1996) *Biochemistry 35*, 1037−1045.
18. Binnig, G., Quate, C. F., and Gerber, Ch. (1986) *Phys. Rev. Lett. 56*, 930−933.
19. Rinia, H. A., Kik, R. A., Demel, R. A., Snel, M. M. E., Killian, J. A., van der Eerden, J. P. J. M., and de Kruijff, B. (2000) *Biochemistry 39*, 5852−5858.
20. Czajkowsky, D. M., Iwamoto, H., Cover, T. L., and Shao, Z. (1999) *Proc. Natl. Acad. Sci. U.S.A. 96*, 2001−2006.
21. Shao, Z., Mou, J., Czajkowsky, D. M., Yang, J., and Yuan, J.-Y. (1996) *Adv. Phys. 45*, 1−86.
22. Müller, D. J., Fotiadis, D., Scheuring, S., Müller, S. A., and Engel, A. (1999) *Biophys. J. 76*, 1101−1111.
23. Mou, J., Czajkowsky, D. M., and Shao, Z. (1996) *Biochemistry 35*, 3222−3226.
24. Curstedt, T., Johansson, J., Persson, P., Eklund, A., Robertson, B., Löwenadler, B., and Jörnvall, H. (1990) *Proc. Natl. Acad. Sci. U.S.A. 87*, 2985−2989.
25. Oosterlaken-Dijksterhuis, M. A., Haagsman, H. P., van Golde, L. M. G., and Demel, R. A. (1991) *Biochemistry 30*, 10965−10971.
26. de Jongh, H. H. J., Goormaghtigh, E., and Killian, J. A. (1994) *Biochemistry 33*, 14521−14528.
27. Grandbois, M., Clausen-Schauman, H., and Gaub, H. (1998) *Biophys. J. 74*, 2398−2404.
28. Rinia, H. A., Demel, R. A., van der Eerden, J. P. J. M., and de Kruijff, B. (1999) *Biophys. J. 77*, 1683−1693.
29. Janshoff, A., Bong, D. T., Steinem, C., Johnson, J. E., and Ghadiri, M. R. (1999) *Biochemistry 83*, 5328−5336.
30. McElhaney, R. N. (1986) *Biochim. Biophys. Acta 864*, 361−421.
31. Lewis, R. N. A. H., Mak, N., and McElhaney, R. N. (1987) *Biochemistry 26*, 6118−6126.
32. Papahadjopoulos, D., Moscarello, M., Eylar, E. H., and Isac, T. (1975) *Biochim. Biophys. Acta 401*, 317−335.
33. Zhang, Y.-P., Lewis, R. N. A. H., Hodges, R. S., and McElhaney, R. N. (1995) *Biochemistry 34*, 2362−2371.
34. Seul, M., and Andelman, D. (1995) Domain shapes and patterns: the phenomenology of modulated phases. *Science 267*, 476−483.
35. Fang, Y., and Yang, J. (1996) *J. Phys. Chem. 100*, 15614−15619.
36. Killian, J. A., and von Heijne, G. (2000) *Trends Biochem. Sci. 25*, 429−434.
37. De Planque, M. R. R. (2000) Ph.D. Thesis, Utrect University, The Netherlands.
38. van der Eerden, J. P. J. M., Snel, M. M. E., Makkinje, J., van Dijk, A. D. J., and Rinia, H. A. (2001) *J. Cryst. Growth* (submitted for publication).
39. Marsh, D. (1990) *Handbook of Lipid Bilayers*, CRC Press, Boca Raton, FL.

BI011796X